# Theoretical Analysis of Battery SOC Estimation Errors Under Sensor Bias and Variance

Xinfan Lin, *Member, IEEE*

***Abstract*—This paper provides a theoretic and systematic analysis on the battery state of charge (SOC) estimation errors caused by sensor noises. The considered noises include the bias and the variance of both current and voltage sensors. Specifically, the bias and the variance of the SOC estimation error are derived as explicit functions of sensor noises, battery parameters, and observer tuning parameters. The derivation is performed for the Kalman filter, which is the most commonly used method for SOC estimation, and the least squares method. It is found that the observer parameter tuning is subject to a tradeoff between suppressing the estimation bias and variance. Either one of these two errors becomes dominant under different observer parameter ranges. The fundamental estimation error that cannot be mitigated through observer tuning has also been identified. The results have been validated by both simulation and experiment. The obtained theoretical findings are of great practical significance as they could be used to guide sensor selection and observer design, as well as enable online uncertainty management.**

***Index Terms*—Battery, estimation bias and variance, Kalman filter, least squares, sensor noise, state of charge estimation.**

## I. Introduction

BATTERY state of charge (SOC) is the energy storage level of a battery cell or a system. It is one of the most critical battery states that need to be monitored during the battery operation. Knowledge of accurate SOC lays the foundation for battery management functions including power management [1]–[3], charging [4]–[6], and cell balancing [7], [8] among others. Since SOC cannot be measured directly, extensive research efforts have been devoted to developing methods for SOC estimation. The basic method is coulomb counting, which integrates the current over time and divides the integral by the capacity to obtain the SOC [9], [10]. The estimates, however, are easily corrupted by the errors in initial SOC guess and the bias in current sensing. Therefore, the majority of research has been focusing on developing closed-loop estimation methods, which combine a battery model with current and voltage measurement to improve the stability and accuracy of estimation. These methods include the Kalman filter [11]–[16], Luenberger observer [17], voltage inversion [18], moving horizon observer [19], [20], $H_\infty$ observer [21], neural network [14], [22], back-stepping PDE observer [23], Lyapunov-based methods [24], and sliding mode observer [25] among others.

Since current and voltage measurements are routinely used in SOC estimation, sensor noises have become a major source of estimation errors. Sensor noises include both bias and variance. Detecting and countering the voltage and current sensor noises have been explored in many research efforts [11], [26]–[28]. However, it is often impossible to eradicate the sensor noise-induced estimation errors, sometimes not even mitigating it. Regarding sensor variance, algorithms such as the Kalman filter need to assume known noise characteristics and could only alleviate the effect of the sensor noise against that of the process noise. For sensor bias, as pointed out in [26], effective estimation (and hence subsequent bias correction) would require the open-circuit voltage (OCV) of the battery to be nonlinear and the use of nonlinear observers. Even if theoretically feasible, the estimation of sensor noise-induced estimation errors is further complicated by the presence of model and parameter uncertainty [29], [30]. Isolating the effect of sensor noises from uncertainty and making correction is typically very difficult.

Therefore, the ability to evaluate/predict the sensor-noise-induced estimation error is highly desirable. On one hand, it can specify the required sensor accuracy to achieve the desirable estimation accuracy, while, on the other, it can provide guidelines for observer design to reduce estimation errors. In addition, if the sensor noise-induced errors are fundamentally irreducible, the prediction of the estimation error (or its bound) could provide valuable information for robust control.

Some recent works have investigated the impact of measurement noises on battery state/parameter estimation accuracy. In [31] and [32], Ramadesigan *et al.* and Vazquez-Arenas *et al.* calculated the confidence interval of estimates under voltage sensing variance using Monte Carlos simulation and analysis of variance. In [33], Forman *et al.* computed the Cramer–Rao bound for parameter estimation under voltage noise variance. These works mostly focus on numerical analysis under specific sets of input and output data. There has also been some analytic research on this topic recently. The Fisher information matrix for some parameters of a battery model is derived under periodic current input in [34]. More importantly, in [35]–[37], Lin and Stefanopoulou derived the analytic expression for the variance of estimation errors (Cramer–Rao bound) caused

Manuscript received April 2, 2017; revised August 3, 2017, October 10, 2017, November 28, 2017, and December 23, 2017; accepted January 3, 2018. Date of publication January 23, 2018; date of current version May 1, 2018.

The author is with the Department of Mechanical and Aerospace Engineering, University of California, Davis, CA 95616 USA (e-mail: lxflin@ucdavis.edu).

Color versions of one or more of the figures in this paper are available online at http://ieeexplore.ieee.org.

Digital Object Identifier 10.1109/TIE.2018.2795521

by voltage sensing variance. The derivation is performed for generic current input, and both the cases of single-variable and multivariable estimation are investigated. Regarding the impact of both sensor variance and bias, Mendoza *et al.* [28] derive the SOC estimation bias and variance under voltage sensor bias and variance for the least-squares method which is mostly used for offline identification. Nevertheless, systematic and theoretical analysis including both the noises of current and voltage sensors is still missing. The current bias is especially important, since it causes significant SOC drift over time under the baseline coulomb counting method. Furthermore, it is highly desirable to investigate this issue for the Kalman filter, which is the most commonly used method for battery SOC estimation [11], [13], [14], [16], [38].

The unique contributions of this paper include the following three aspects. First, the mean and variance of the SOC estimation error induced by current and voltage sensor bias and variance are derived theoretically. The analytic expressions present the estimation bias and variance as explicit functions of sensing bias and variance, battery parameters, and observer tuning parameters. Preliminary results have been published in a previous paper [39]. Second, the derivation is performed for two estimation methods, including the Kalman filter and the least-squares method. It is noted that the Kalman filter usually assumes zero-mean and white sensor noise, which is not necessarily in accordance with reality due to the common presence of sensor bias. This paper will quantify the SOC estimation errors caused by both sensing variance and bias to evaluate the performance of Kalman filter in practice. The results obtained can be extended to a general class of observers, namely the recursive observer with output error injection which further include the Luenberger observer [17], [40]. Third, it is found that there is a tradeoff regarding observer tuning between suppressing the bias and the variance of SOC estimation. Adjusting observer parameters, such as the gain of the Kalman filter and the window size of the least-squares method, will typically reduce one error characteristic (either bias or variance) at the cost of increasing the other. As a result, the bias or the variance becomes the dominant error type in different observer parameter ranges. It is also found that there exists a fundamental estimation bias that cannot be mitigated through observer tuning.

## II. Model and Problem Formulation

In this section, the equivalent circuit model [41]–[43], which will be used for derivation, is introduced. The SOC estimation error and sensor noises are defined subsequently.

### A. Equivalent Circuit Battery Model

The schematic of an equivalent circuit battery model is shown in Fig. 1. This model uses a series resistance $R_0$ to represent the battery ohmic resistance, and multiple *R–C* pairs to capture the transient battery dynamics such as the charge transfer kinetics, the lithium ion diffusion, and the solid/electrolyte interface (SEI) dynamics. The model also includes an SOC-dependent OCV which reflects the static battery voltage under no current input.

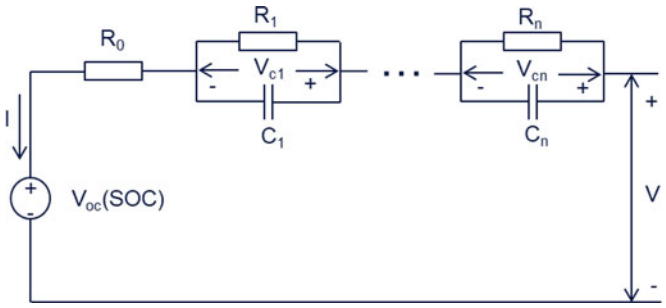


Fig. 1. Equivalent circuit model.

The discrete-time model governing equations take the following form:

$$\mathrm{SOC}_{k+1} = \mathrm{SOC}_k + \frac{I_k \Delta t}{C_{\mathrm{bat}}} \tag{1a}$$

$$V_{cj,k+1} = e^{-\frac{\Delta t}{R_j C_j}} V_{cj,k} + R_j \left(1 - e^{-\frac{\Delta t}{R_j C_j}}\right) I_k, \tag{1b}$$

$$V_k = g(\mathrm{SOC}_k) + \sum_{j}^{n} V_{cj,k} + I_k R_0 \tag{1c}$$

where the subscript $k$ denotes the time step, $I$ is the current, $\Delta t$ is the sampling period, $C_{\mathrm{bat}}$ is the capacity, $V_{cj}$ is the voltage of the equivalent circuit pair $j$, $R_j$ and $C_j$ are the resistance and capacitance of each pair, $g(\mathrm{SOC}_k)$ is the nonlinear OCV function, and $R_0$ is the ohmic resistance. It is noted that battery dynamics are dependent on temperature [44], [45]. Therefore, in order to have a high-fidelity model, the parameters need to be treated as varying with temperature as in [43] and [46]. If the temperature-dependency of the parameters is not considered, there will be a parameter mismatch/model uncertainty that would also corrupt SOC estimation. The SOC estimation error induced by parameter mismatch has been studied in a previous work [29], and it is the focus of this work to investigate the estimation error caused by sensor noises.

The equivalent circuit model is used in this paper for two reasons. First, it is the most commonly used model for the estimation and control of battery [41]–[43], [47] and other energy storage systems such as ultracapacitor [48], [49]. Second, it is closely related with other battery models including the single particle model [13], [50], the impedance model [51]–[53], and the electrochemical model [54]. These models can be converted to the equivalent circuit model using model reduction or transformation techniques. For example, it is shown in [52] that the equivalent circuit model can be converted from a single particle model by Pade approximation, which itself is simplified from a first principle battery electrochemical model [54]. In [51], Dong *et al.* represented the battery impedance identified from electrochemical impedance spectroscopy in the form of an equivalent circuit model. The constant phase elements, which are used to model the dynamics of the SEI film, the charge transfer kinetics, and the Warburg diffusion impedance, are approximated by a series of *R–C* pairs. However, the number of *R–C* pairs needed

for high-fidelity approximation can be significant, which is a main limitation of the equivalent circuit model.

### B. Definition of Sensor Bias, Sensor Variance, and SOC Estimation Error

This work considers both current and voltage noises. Both noises include a constant bias and a randomly varying part,

$$\begin{aligned} V_k^m &= V_k^* - \Delta V - \delta V_k, \\ I_k^m &= I_k^* - \Delta I - \delta I_k \end{aligned} \tag{2}$$

where the superscript $^m$ denotes the measured value of respective variables, $^*$ denotes the true value, $\Delta V$ and $\Delta I$ are the constant voltage and current biases, and $\delta V$ and $\delta I$ are the random part of the noises. The random noises are independent and identically distributed (i.i.d.) among samples with zero mean and constant variance $\sigma_V^2$ and $\sigma_I^2$ as follows:

$$\begin{aligned} E(\delta V) = 0, \quad \sigma^2(\delta V) = \sigma_V^2 \\ E(\delta I) = 0, \quad \sigma^2(\delta I) = \sigma_I^2. \end{aligned} \tag{3}$$

It is noted that the biases $\Delta V$ and $\Delta I$ can vary slowly over time in reality. In this paper, we consider such variation as slower than the dynamics of the observer so that they can be treated as constant during the derivation.

The goal of estimation is to use the model and the noisy measurements $V_k^m$ and $I_k^m$ to determine SOC. In the presence of sensor noises (and model uncertainty), the estimate $S\hat{O}C$ will not be the same as the true value SOC$^*$, and the resulted estimation error is defined as

$$\Delta \text{SOC}_k = \text{SOC}_k^* - S\hat{O}C_k. \tag{4}$$

The SOC estimation errors induced by model uncertainty, such as parameter mismatch and model reduction, have been investigated in [29] and [30], respectively. This paper focuses on exploring $\Delta$SOC under sensor noises.

## III. Theoretical Derivation of Sensor-Noise-Induced SOC Estimation Error

In this section, the analytic expressions of the SOC estimation error induced by voltage and current bias and variance are derived for two estimation methods, namely the least-squares method and the Kalman filter.

### A. SOC Estimation Error Under Least Squares

The least-squares method finds an estimate that minimizes the sum of the squares of the output errors over samples.

Suppose we want to estimate battery SOC at time instant $k$, $\text{SOC}_k$, based on $N$ past current and voltage measurements

$$\begin{aligned} \mathbf{I^m} &= \left[ I_{k-N+1}^m,\ I_{k-N+2}^m,\ \ldots,\ I_l^m,\ \ldots,\ I_k^m \right]^T \\ \mathbf{V^m} &= \left[ V_{k-N+1}^m,\ V_{k-N+2}^m,\ \ldots,\ V_l^m,\ \ldots,\ V_k^m \right]^T. \end{aligned} \tag{5}$$

The least-squares estimation problem is defined as

$$\min_{S\hat{O}C_k} J = \frac{1}{2} \sum_{l=k-N+1}^{k} (V_l^m - \hat{V}_l)^2. \tag{6}$$

The estimate $S\hat{O}C_k$ can be found by solving $\frac{\partial J}{\partial S\hat{O}C_k} = 0$, which gives

$$\sum_{l=k-N+1}^{k} (V_l^m - \hat{V}_l) \frac{\partial (V_l^m - \hat{V}_l)}{\partial S\hat{O}C_k} = 0. \tag{7}$$

The key of derivation is to find the analytic expressions for $V_l^m - \hat{V}_l$ and $\frac{\partial (V_l^m - \hat{V}_l)}{\partial S\hat{O}C_k}$, and solve for $S\hat{O}C_k$ symbolically.

The voltage measurement $V_l^m$ can be written as

$$\begin{aligned} V_l^m = g(\text{SOC}_k^*) - \sum_{i=l}^{k-1} \frac{\alpha_i I_i^* \Delta t}{C_{\text{bat}}} + \sum_{j}^{n} V_{cj,l}^* \\ + I_l^* R_0 - \Delta V - \delta V_l \end{aligned} \tag{8}$$

based on (1) and (2), where $\alpha_i$ is the slope of $g(\text{SOC})$ at time step $i$. In a similar way, the voltage estimation $\hat{V}_l$ can be obtained as

$$\begin{aligned} \hat{V}_l = g(S\hat{O}C_k) - \sum_{i=l}^{k-1} \frac{\hat{\alpha}_i (I_i^* - \Delta I - \delta I_i) \Delta t}{C_{\text{bat}}} + \sum_{j}^{n} \hat{V}_{cj,l} \\ + (I_l^* - \Delta I - \delta I_l) R_0. \end{aligned} \tag{9}$$

Two assumptions are then made here. First, it is assumed that $\sum_j^n V_{cj,l}^* = \sum_j^n \hat{V}_{cj,l}$ since the difference between the two caused by current noise is minimal. Second, $\alpha$ and $\hat{\alpha}$ are assumed to be equal, which holds in most cases since the battery OCV is typically piecewise linear and $S\hat{O}C_k$ is usually not too far away from $\text{SOC}_k^*$. The assumptions will be verified later in simulation and experiment. The voltage error $V_l^m - \hat{V}_l$ can then be obtained by subtracting (9) from (8),

$$\begin{aligned} V_l^m - \hat{V}_l = g(\text{SOC}_k^*) - g(S\hat{O}C_k) - \sum_{i=l}^{k-1} \frac{\alpha_i (\Delta I + \delta I_i) \Delta t}{C_{\text{bat}}} \\ + \Delta I R_0 + \delta I_l R_0 - \Delta V - \delta V_l. \end{aligned} \tag{10}$$

Furthermore, based on the second assumption, we also have

$$\begin{aligned} g(\text{SOC}_k^*) - g(S\hat{O}C_k) &= \alpha_k (\text{SOC}_k^* - S\hat{O}C_k) \\ &= \alpha_k \Delta \text{SOC}_k. \end{aligned} \tag{11}$$

Hence, (10) becomes

$$\begin{aligned} V_l^m - \hat{V}_l = \alpha_k \Delta\, \text{SOC}_k - \sum_{i=l}^{k-1} \frac{\alpha_i (\Delta I + \delta I_i) \Delta t}{C_{\text{bat}}} \\ + \Delta I R_0 + \delta I_l R_0 - \Delta V - \delta V_l. \end{aligned} \tag{12}$$

Finally, the analytic expression of $\Delta\text{SOC}_k$ is obtained by substituting (12) into (7) and solving (7) as follows:

$$\Delta\text{SOC}_k = \frac{\Delta V - \Delta I R_0}{\alpha_k} + \frac{\sum_{l=k-N+1}^{k} \delta V_l}{N\alpha_k} - \frac{R_0 \sum_{l}^{k} \delta I_l}{N\alpha_k} + \frac{\Delta I \Delta t}{N C_{\text{bat}} \alpha_k} \sum_{l=k-N+1}^{k} \sum_{i=l}^{k-1} \alpha_i + \frac{\Delta t}{N C_{\text{bat}} \alpha_k} \sum_{l=k-N+1}^{k} \sum_{i=l}^{k-1} \alpha_i \delta I_i. \tag{13}$$

Since $\delta V$ and $\delta I$ are i.i.d. zero-mean random variables with variances $\sigma_V^2$ and $\sigma_I^2$, the expectation and variance of $\Delta\text{SOC}_k$ are

$$E(\Delta\text{SOC}_k) = \frac{\Delta V - \Delta I R_0}{\alpha_k} + \frac{\Delta I \Delta t}{N C_{\text{bat}} \alpha_k} \sum_{l=k-N+1}^{k} \sum_{i=l}^{k-1} \alpha_i$$

$$\sigma^2(\Delta\text{SOC}_k) = \frac{\sigma_V^2}{N\alpha_k^2} + \frac{R_0^2 \sigma_I^2}{N^2 \alpha_k^2} + \frac{\sigma_I^2}{N^2 \alpha_k^2} \sum_{l=k-N+1}^{k-1} \left[ (l-k+N) \frac{\alpha_l \Delta t}{C_{\text{bat}}} - R_0 \right]^2. \tag{14}$$

The error characteristics under other assumptions of noise statistics, such as time varying (nonstationary) noises, can also be derived based on the generic expression (13).

Furthermore, if $g(\text{SOC})$ is linear with a constant slope $\alpha$ (at least within the estimation window) and $N$ is large enough, (14) is reduced to

$$E(\Delta\text{SOC}_k) = \frac{\Delta V}{\alpha} - \frac{\Delta I R_0}{\alpha} + N \frac{\Delta I \Delta t}{2 C_{\text{bat}}}$$

$$\sigma^2(\Delta\text{SOC}_k) = \frac{\sigma_V^2}{N\alpha^2} + \frac{R_0^2 \sigma_I^2}{N\alpha^2} + \frac{N}{3} \frac{\Delta t^2 \sigma_I^2}{C_{\text{bat}}^2} - \frac{\Delta t R_0}{2\alpha C_{\text{bat}}} \sigma_I^2. \tag{15}$$

Some interesting observations can be made from (15) as follows:

1) The SOC estimation bias $E(\Delta\text{SOC}_k)$ includes three terms. The first term $\frac{\Delta V}{\alpha}$ captures the impact of voltage bias $\Delta V$ on $E(\Delta\text{SOC}_k)$, acting through the slope of OCV $\alpha$. Similarly, the second term $-\frac{\Delta I R_0}{\alpha}$ describes the impact of $\Delta I$ through the resistance $R_0$ and $\alpha$. The third term $N\frac{\Delta I \Delta t}{2C_{\text{bat}}}$ accounts for the accumulation of $\Delta I$ over samples due to current integration.
2) The estimation variance $\sigma^2(\Delta\text{SOC}_k)$ includes four terms. The first term $\frac{\sigma_V^2}{N\alpha^2}$ reflects the impact of voltage variance $\sigma_V^2$ on SOC estimation through $\alpha$. The remaining terms capture the impact of current variance $\sigma_I^2$. On one hand, $\delta I$ will affect the voltage estimation through $\delta I R_0$ and hence cause SOC estimation error through $\alpha$, giving the second term $\frac{R_0^2 \sigma_I^2}{N\alpha^2}$. On the other hand, $\delta I$ will also affect the SOC calculation through current integration, which renders the third term $\frac{N}{3}\frac{\Delta t^2 \sigma_I^2}{C_{\text{bat}}^2}$. Since the second and the third terms originate from the same current noise $\delta I$, they are not independent. The fourth term $-\frac{\Delta t R_0}{2\alpha C_{\text{bat}}}\sigma_I^2$ accounts for the correlation between them.
3) Key factors that contribute to the SOC estimation error can be studied based on the derived expressions. High OCV slope $\alpha$ could reduce both estimation bias $E(\Delta\text{SOC})$ and variances $\sigma^2(\Delta\text{SOC})$ by enhancing the SOC sensitivity. More importantly, there is a tradeoff regarding tuning the number of data points $N$ in the estimation window. Increasing $N$ will reduce $\sigma^2(\Delta\text{SOC})$ but at the cost of increasing $E(\Delta\text{SOC})$.[1] Tuning of $N$ needs to consider this tradeoff. It is also noted that there is a fundamental bias, $\frac{\Delta V}{\alpha} - \frac{\Delta I R_0}{\alpha}$, which cannot be reduced by tuning $N$. The $E(\Delta\text{SOC})$ and $\sigma^2(\Delta\text{SOC})$ derived here will be reduce to the form in [28], when $\Delta I$ and $\sigma_I^2$ are not considered.

## B. SOC Estimation Error Under Kalman Filter

The Kalman filter estimates the battery SOC in two steps, namely the prediction step and the update step.

At each time instant $k$, SOC is first predicted based on the model (1a) and the measured current,

$$\hat{SOC}_k^- = \hat{SOC}_{k-1} + \frac{I_{k-1}^m \Delta t}{C_{\text{bat}}},$$
$$\hat{P}_k^- = \hat{P}_{k-1} + Q \tag{16}$$

where $\hat{P}$ is the estimated SOC error variance, $Q$ is the (assumed) process noise variance, and the superscript $^-$ denotes the model prediction value. Next, the SOC estimate is updated based on the voltage error as follows:

$$\hat{SOC}_k = \hat{SOC}_k^- + L_k (V_k^m - \hat{V}_k^-). \tag{17}$$

The feedback gain $L_k$ is calculated as

$$L_k = \hat{P}_k^- \hat{\alpha}_k^T (\hat{\alpha}_k \hat{P}_k^- \hat{\alpha}_k^T + R)^{-1} \tag{18}$$

where $R$ is the (assumed) measurement noise variance. Meanwhile, $\hat{P}$ is also updated as

$$\hat{P}_k = (1 - L_k \hat{\alpha}_k) \hat{P}_k^-. \tag{19}$$

In (18) and (19), $\hat{\alpha}_k$ is the gradient of $g(\text{SOC})$ evaluated at $\hat{SOC}_k^-$,

$$\hat{\alpha}_k = \left. \frac{\partial g}{\partial \text{SOC}} \right|_{\hat{SOC}_k^-}. \tag{20}$$

The recursive expression of $\hat{SOC}_k$ can be obtained by combining (16) and (17) as

$$\hat{SOC}_k = \hat{SOC}_{k-1} + \frac{I_{k-1}^m \Delta t}{C_{\text{bat}}} + L_k (V_k^m - \hat{V}_k^-) \tag{21}$$

[1] To be exact, increasing $N$ will reduce 1) the $\sigma^2(\Delta\text{SOC})$ caused by $\sigma_V^2$ and 2) the $\sigma^2(\Delta\text{SOC})$ caused by $\sigma_I^2$ through $R_0$, but with increased $E(\Delta\text{SOC})$ and 3) $\sigma^2(\Delta\text{SOC})$ caused by $\sigma_I^2$ through current integration. It turns out that for actual lithium ion battery chemistry, 1) is usually the dominant component of $\sigma^2(\Delta\text{SOC})$ as compared to 2) and 3). Therefore, the statement can be simplified to the way in the main paragraph. This will also be verified later in Section V.

where

$$\hat{V}_k^m = g(\mathrm{SOC}_k^*) + \sum_j^n V_{cj,k}^* + I_k^* R_0 - \Delta V - \delta V_k,$$

$$\hat{V}_k^- = g(S\hat{O}C_k^-) + \sum_j^n \hat{V}_{cj,k} + (I_k^* - \Delta I - \delta I_k)R_0. \quad (22)$$

The voltage error is therefore

$$V_k^m - \hat{V}_k^- = g(\mathrm{SOC}_k^*) - g(S\hat{O}C_k^-) + (\Delta I + \delta I_k)R_0 - \Delta V - \delta V_k. \quad (23)$$

Again, it is assumed that $\sum_j^n V_{cj,l}^* = \sum_j^n \hat{V}_{cj,l}$ since the difference of the two caused by current noise is minimal. We then apply the approximation

$$\begin{aligned} &g(\mathrm{SOC}_k^*) - g(S\hat{O}C_k^-) \\ &= g\left(\mathrm{SOC}_{k-1}^* + \frac{I_{k-1}^*\Delta t}{C_{\mathrm{bat}}}\right) - g\left(S\hat{O}C_{k-1} + \frac{I_{k-1}^m \Delta t}{C_{\mathrm{bat}}}\right) \\ &\approx g(\mathrm{SOC}_{k-1}^*) + \alpha_k \frac{I_{k-1}^*\Delta t}{C_{\mathrm{bat}}} - g\left(S\hat{O}C_{k-1}\right) - \alpha_k \frac{I_{k-1}^m \Delta t}{C_{\mathrm{bat}}} \\ &\approx \alpha_k \Delta \mathrm{SOC}_{k-1} + \alpha_k \frac{(\Delta I + \delta I_{k-1})\Delta t}{C_{\mathrm{bat}}} \end{aligned} \quad (24)$$

which holds when $S\hat{O}C_k$ is not too far away from $\mathrm{SOC}_k^*$.

By substituting (23) and (24) into (21), we have

$$\begin{aligned} S\hat{O}C_k = S\hat{O}C_{k-1} + \frac{I_{k-1}^m \Delta t}{C_{\mathrm{bat}}} + L_k\Bigg(&\alpha_k \Delta \mathrm{SOC}_{k-1} \\ &+ \alpha_k \frac{(\Delta I + \delta I_{k-1})\Delta t}{C_{\mathrm{bat}}} + (\Delta I + \delta I_k)R_0 - \Delta V - \delta V_k\Bigg). \end{aligned} \quad (25)$$

Meanwhile, the true SOC is

$$\mathrm{SOC}_k^* = \mathrm{SOC}_{k-1}^* + \frac{I_{k-1}^*\Delta t}{C_{\mathrm{bat}}}. \quad (26)$$

The recursive expression of the estimation error $\Delta\mathrm{SOC} = \mathrm{SOC}^* - S\hat{O}C$ can be obtained by subtracting (25) from (26) as follows:

$$\begin{aligned} \Delta \mathrm{SOC}_k = &(1 - \alpha_k L_k)\Delta SOC_{k-1} \\ &+ (1 - \alpha_k L_k)\frac{(\Delta I + \delta I_{k-1})\Delta t}{C_{\mathrm{bat}}} \\ &+ L_k(\Delta V + \delta V_k - (\Delta I + \delta I_k)R_0). \end{aligned} \quad (27)$$

When the initial SOC estimation error is $\Delta\mathrm{SOC}_0$, the solution of $\Delta\mathrm{SOC}_k$ is

$$\begin{aligned} \Delta \mathrm{SOC}_k = &\prod_{i=1}^k (1 - \alpha_i L_i)\Delta \mathrm{SOC}_0 \\ &+ \sum_{i=1}^k \Bigg\{ \prod_{m=i+1}^k (1 - \alpha_m L_m)\Bigg[(1 - \alpha_i L_i)\frac{(\Delta I + \delta I_{i-1})\Delta t}{C_{\mathrm{bat}}} \\ &+ L_i(\Delta V + \delta V_i - (\Delta I + \delta I_i)R_0)\Bigg]\Bigg\}. \end{aligned} \quad (28)$$

The expectation and variance of $\Delta\mathrm{SOC}_k$ are hence

$$\begin{aligned} E(\Delta \mathrm{SOC}_k) = &\prod_i^k (1 - \alpha_i L_i)\Delta \mathrm{SOC}_0 \\ &+ \sum_{i=1}^k \Bigg\{ \left[(1 - \alpha_i L_i)\frac{\Delta I \Delta t}{C_{\mathrm{bat}}} + L_i(\Delta V - \Delta I R_0)\right] \\ &\cdot \prod_{m=i+1}^k (1 - \alpha_m L_m)\Bigg\}. \\ \sigma^2(\Delta \mathrm{SOC}_k) = &\sum_{i=1}^k \Bigg\{ L_i \prod_{m=i+1}^k (1 - \alpha_m L_m)\Bigg\}^2 \sigma_V^2 \\ &+ \sum_{i=0}^{k-1} \Bigg\{ \left(\frac{\Delta t}{C_{\mathrm{bat}}} - L_i R_0\right) \prod_{m=i+1}^k (1 - \alpha_m L_m)\Bigg\}^2 \sigma_I^2 \\ &+ L_k^2 R_0^2 \sigma_I^2. \end{aligned} \quad (29)$$

It is noted that for many lithium ion battery chemistries, the OCV is approximately piece-wise linear. For example, the OCV slope of the NMC battery is close to a constant $\alpha = 0.65$ mV/1% SOC between the nominal operating range of 10–100% SOC [35]. In this case, it can be proved that the feedback gain will converge to a constant $L$ in the range $0 < L < \frac{1}{\alpha}$. Therefore, when $k \to \infty$, (29) will converge to

$$\begin{aligned} E(\Delta \mathrm{SOC}) \to &\frac{\Delta V}{\alpha} - \frac{\Delta I R_0}{\alpha} + \left(\frac{1}{\alpha L} - 1\right)\frac{\Delta I \Delta t}{C_{\mathrm{bat}}} \\ \sigma^2(\Delta \mathrm{SOC}) \to &\frac{1}{\frac{2\alpha}{L} - \alpha^2}\sigma_V^2 + L^2 R_0^2 \sigma_I^2 \\ &+ \frac{(1 - \alpha L)\left(\frac{\Delta t}{C_{\mathrm{bat}}} - L R_0\right)^2}{2\alpha L - \alpha^2 L^2}\sigma_I^2 \end{aligned} \quad (30)$$

which represent the asymptotic bias and variance of the SOC estimation error induced by $\Delta V$, $\Delta I$, $\delta I$, and $\delta V$.

Observations can be made as follows:

1) The asymptotic estimation bias $E(\Delta\mathrm{SOC})$ includes three terms. The first two terms $\frac{\Delta V}{\alpha}$ and $-\frac{\Delta I R_0}{\alpha}$ are the same as those of the least-squares method in (15). They account for the estimation bias caused by voltage bias through OCV and that caused by current bias through $R_0$ and OCV. The third term $(\frac{1}{\alpha L} - 1)\frac{\Delta I \Delta t}{C_{\mathrm{bat}}}$ quantifies the estimation bias induced by current bias through current integration.
2) The asymptotic estimation variance $\sigma^2(\Delta\mathrm{SOC})$ involves three terms. The first term $\frac{1}{\frac{2\alpha}{L} - \alpha^2}\sigma_V^2$ captures the effect of voltage variance $\sigma_V^2$ through $\alpha$. The second term $L^2 R_0^2 \sigma_I^2$ quantifies the contribution of $\sigma_I^2$ through $R_0$. The third term $\frac{(1-\alpha L)\left(\frac{\Delta t}{C_{\mathrm{bat}}} - L R_0\right)^2}{2\alpha L - \alpha^2 L^2}\sigma_I^2$ accounts for the estimation variance induced by $\sigma_I^2$ through current integration. The second and the third terms are correlated, and the correlation is reflected in the numerator of the third term, namely $\frac{\Delta t}{C_{\mathrm{bat}}} - L R_0$.

TABLE I
(ASYMPTOTIC) SOC ESTIMATION BIAS AND VARIANCE UNDER CURRENT AND VOLTAGE NOISES

| Method | $E(\Delta\text{SOC})$ | $\sigma^2(\Delta\text{SOC})$ |
|---|---|---|
| Least Squares | $\frac{\Delta V}{\alpha} - \frac{R_0}{\alpha}\Delta I + N\frac{\Delta t}{2C_{\text{bat}}}\Delta I$ | $\frac{\sigma_V^2}{N\alpha^2} + \frac{R_0^2}{N\alpha^2}\sigma_I^2 + \frac{N}{3}\frac{\Delta t^2}{C_{\text{bat}}^2}\sigma_I^2 - \frac{\Delta t R_0}{2\alpha C_{\text{bat}}}\sigma_I^2$ |
| Kalman Filter | $\frac{\Delta V}{\alpha} - \frac{R_0}{\alpha}\Delta I + \frac{(\frac{1}{\alpha L}-1)\Delta t}{C_{\text{bat}}}\Delta I$ | $\frac{1}{\frac{2\alpha}{L}-\alpha^2}\sigma_V^2 + L^2R_0^2\sigma_I^2 + \frac{(1-\alpha L)\left(\frac{\Delta t}{C_{\text{bat}}}-LR_0\right)^2}{2\alpha L-\alpha^2L^2}\sigma_I^2$ |

3) Key contributing factors of the estimation error can be identified. High OCV slope $\alpha$ improves the estimation accuracy as it reduces both $E(\Delta\text{SOC})$ and $\sigma^2(\Delta\text{SOC})$. As for the Kalman filter gain tuning, there is a tradeoff between suppressing $E(\Delta\text{SOC})$ and $\sigma^2(\Delta\text{SOC})$, similar to the window size tuning for the least-squares method. Using high gain $L$ will reduce the $E(\Delta\text{SOC})$ induced by $\Delta I$ but increase the $\sigma^2(\Delta\text{SOC})$ caused by $\sigma_V^2$ and $\sigma_I^2$. The tradeoff relationship can be used as a guideline for observer design. Moreover, there is also a fundamental bias $\frac{\Delta V}{\alpha} - \frac{\Delta I R_0}{\alpha}$, same as that of the least-squares method, which cannot be mitigated through gain tuning.

The derived SOC estimation bias $E(\Delta\text{SOC})$ and variance $\sigma^2(\Delta\text{SOC})$ for the least-squares method and the Kalman filter are summarized in Table I.

### C. Comparison of Derived Estimation Error Variance With Cramer–Rao Bound

In a previous paper [35], the Cramer–Rao bound of battery SOC estimation was derived under the voltage sensing variance. The Cramer–Rao bound indicates the best-case estimation error variance for the unbiased estimators. It would be interesting to compare that with the variance of biased estimation derived in this paper.

The Cramer–Rao bound under only $\sigma_V^2$ is $\frac{\sigma_V^2}{N\alpha^2}$ as derived in [35]. It is identical to the derived $\sigma^2(\Delta\text{SOC})$ for the least-squares method in (15) when $\sigma_I^2 = 0$. Regarding the Kalman filter, the asymptotic $\sigma^2(\Delta\text{SOC})$ is $\frac{1}{\frac{2\alpha}{L}-\alpha^2}\sigma_V^2$ under only $\sigma_V^2$ and no $\sigma_I^2$, and the best-case value is 0 when $L = 0$. It is noted that the asymptotic variance is attained when time approaches infinity. This scenario is equivalent to $N = \infty$ for the Cramer–Rao bound. In this case, the Cramer-Rao bound is 0, which is equal to the best-case variance of the Kalman filter. Therefore, it is shown that the derived $\sigma^2(\Delta\text{SOC})$ under biased estimation (caused by sensing bias) agrees with the Cramer–Rao bound for unbiased estimation.

## IV. VALIDATION BY SIMULATION AND EXPERIMENT

In this section, the derived analytic expressions of the SOC estimation error are validated based on the simulation and experimental data of an actual lithium ion battery. The battery under investigation is a Lithium-Nickel-Manganese-Cobalt-Oxide (NMC) cell, which is designed for electric vehicle applications. The battery is of prismatic geometry with dimensions 120 × 85 × 12.7 mm, and has a nominal capacity of 5 Ah. A dynamic electric vehicle operation cycle is used for validation. The simulation analysis is capable of demonstrating the estimation errors purely caused by the sensor noises, while the experiment analysis shows the combined errors induced by both the sensor noises and the model uncertainty.

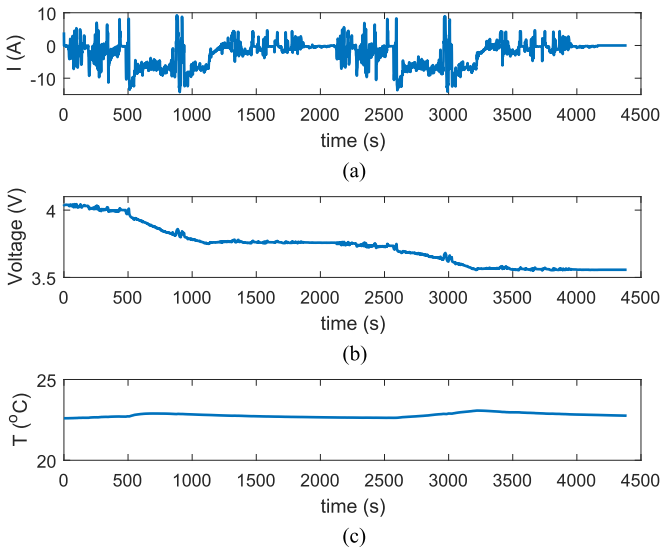


Fig. 2. (a) Current, (b) voltage, and (c) temperature profiles of NMC battery under simulation.

### A. Simulation Verification

The current cycle used for verification is shown in Fig. 2(a). This cycle discharges the battery SOC from around 95% to 20%, which is the normal operating range of the plug-in electric vehicle. During simulation, the voltage response is generated by a battery model as shown in Fig. 2(b). This model is developed and parameterized in [46] for the NMC battery. The model parameters are dependent on temperature and SOC, and this model also includes a thermal submodel capturing the temperature dynamics of the battery. The temperature response during simulation is plotted in Fig. 2(c). Sensor noises have been added to emulate the noisy measurements in practice. Given the voltage measurement range of 0–5 V and the current range of −50 A to +50 A (−10 C to +10 C), the voltage and current noises are assumed to be 0.2% of the full range,

$$\Delta V = 10\text{ mV}, \quad \sigma_V = 10\text{ mV},$$
$$\Delta I = 0.2\text{ A}, \quad \sigma_I = 0.2\text{ A}. \tag{31}$$

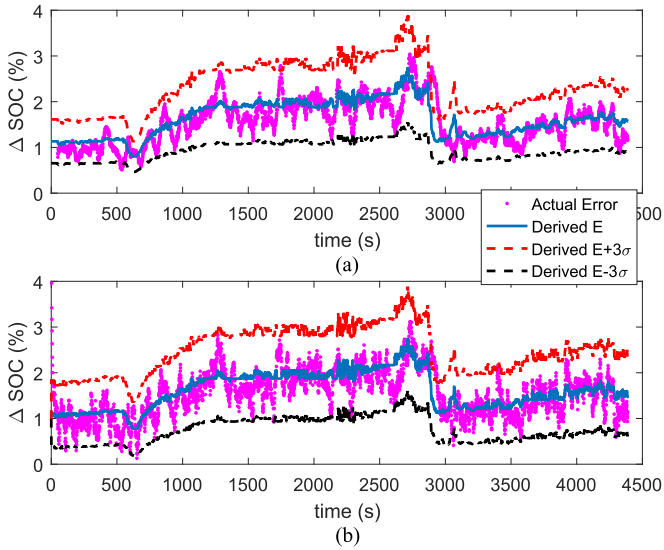


Fig. 3. Simulation verification: Comparison of SOC estimation errors with derived mean and variance under simulation. (a) Least Squares and (b) Kalman Filter.

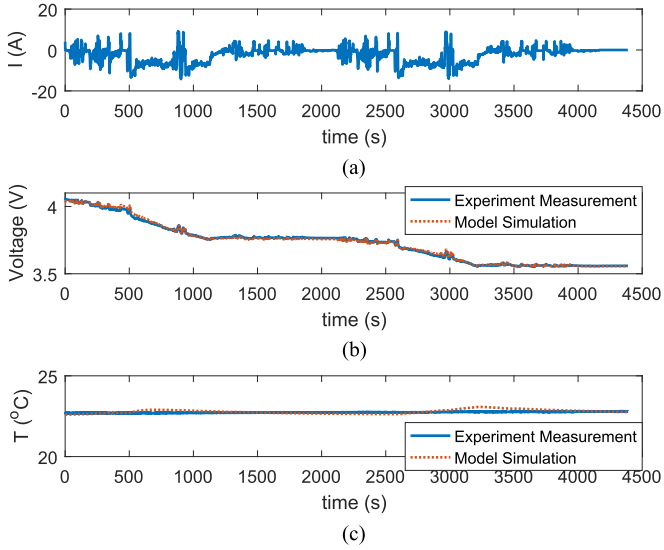


Fig. 4. (a) Current, (b) voltage, and (c) temperature profiles of NMC battery under experiment.

Regarding the estimation algorithm, the Kalman filter and the least-squares method are designed based on the same model that is used to generate the voltage data. Therefore, the resultant SOC estimation error seen in simulation is purely caused by sensor noises but not other disturbances such as model uncertainty. The actual initial SOC is set to 94%, while the initial guess of the observers is 89%. The window size $N$ of the least-squares method is set to 50, and the variances of the Kalman filter are $Q = 0.1$ and $R = 10$, respectively. In addition, the observers compute the *R–C* pair voltage $V_c$ based on the emulated current measurements with noises but not the actual values. In this way, the deviation of $V_c$ caused by current noise is preserved, and the assumption made during the derivation that the impact of the sensor-noise-induced $V_c$ deviation on SOC estimation is negligible can be tested.

The goal of simulation verification is to examine how well the derived expressions of the asymptotic bias and variance could capture the estimation errors that vary in real time due to the changing battery parameters and observer dynamics. The theoretic SOC estimation bias $E(\Delta\text{SOC})$ and variance $\sigma^2(\Delta\text{SOC})$ are calculated based on (15) and (30) using the time-varying OCV slope $\hat{\alpha}$ (at the estimated SOC) and gain $L$. The estimation errors obtained from simulation are plotted against the derived $E(\Delta\text{SOC}) \pm 3\sigma(\Delta\text{SOC})$ in Fig. 3(a) for the least-squares method and in Fig. 3(b) for the Kalman filter. It can be seen that the error characteristics predicted by the derivation match the actual errors very well. The derived $E(\Delta\text{SOC})$ follows the trend of the estimation errors closely, and $E(\Delta\text{SOC}) \pm 3\sigma(\Delta\text{SOC})$ bound the error spread tightly. The deviation of $V_c$ caused by the current noise, which is neglected during the derivation, does not lead to a significant mismatch between the actual and the theoretic SOC estimation error. The verification results demonstrate that although (15) and (30) are derived under the assumption of constant OCV slope and converged observer gain, they could approximate the dynamic error characteristics well enough to be used for computation conveniently in practice.

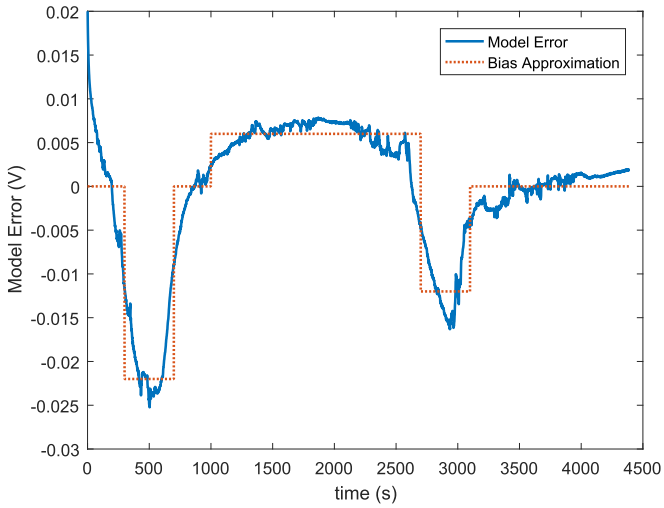


Fig. 5. Voltage error between measurement and model prediction and its approximation as bias.

## B. Experiment Validation

Experiments have also been conducted for validation. An NMC battery was cycled with a Bitrode FTV-1 Cycler using the same current profile in simulation. The sampling frequency of the current, voltage, and temperature measurement is 1 Hz. The measurement data are plotted by the solid lines in Fig. 4 with current in (a), voltage in (b), and temperature in (c). The voltage and temperature responses obtained from model simulation are also plotted in Fig. 4(b) and (c) by the dotted lines for comparison. Certain difference can be observed between the measured and the model-predicted voltage, which is shown in Fig. 5. Such difference includes both model uncertainty and measurement

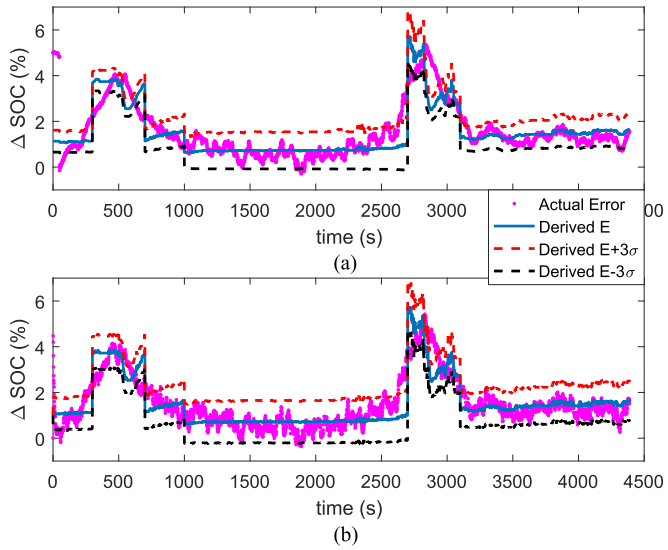


Fig. 6. Experiment validation: Comparison of SOC estimation errors with derived mean and variance under experiment. (a) Least Squares and (b) Kalman Filter.

noises in principle. Due to the high accuracy of the laboratory-grade cycler (much higher than that of the practical sensors per specifications and thanks to regular maintenance), this voltage mismatch can be considered as mostly model uncertainty. The uncertainty is caused by potential mismatch in model parameters and uncaptured battery dynamics such as hysteresis. To emulate the noise level of the practical sensors, random noises with specs in (31) are injected into the measurement data. Furthermore, the voltage mismatch shown in Fig. 5, whether caused by sensor noise or model uncertainty, can be considered as an additive disturbance imposed on the actual battery voltage. Therefore, the mismatch will cause SOC estimation error in the same way as the voltage noise, and the error can be quantified based on the analytic expressions derived in this paper. As seen in Fig. 5, the mismatch can be approximated as piecewise constant biases, i.e., –22 mV between 300 and 700 s, 6 mV between 1000 and 2700 s, and –12 mV between 2700 and 3100 s. These biases will be taken into account as part of $\Delta V$ when calculating the theoretic estimation error based on (15) and (30).

For validation, the actual battery SOC is calculated based on current integration using the (clean) current measurement, and the SOC estimates are generated by the least-squares method and the Kalman filter using the noisy current and voltage data and the model with uncertainty. The tuning parameters and initial guess of the observers take the same values as in simulation. The actual SOC estimation errors are calculated as the difference of the actual and the estimated SOC. The theoretic SOC estimation errors are computed based on (15) and (30) considering both the injected sensor noises and the (piecewise approximation of the) model uncertainty shown in Fig. 5. The actual and the theoretic estimation errors are then compared for validation, as plotted in Fig. 6. It can be seen that the theoretic bias and error bounds match the actual error characteristics well overall. The trend of the estimation error is captured by the derived $E(\Delta\text{SOC})$, and most of the errors fall within the theoretic $\pm 3\sigma(\Delta\text{SOC})$ bounds. There are some mismatches between $0-700$ s and around 2700 s possibly due to the model uncertainty that has not been fully accounted for and the transient error dynamics.

Based on the results shown above, the SOC estimation error remains bounded and does not grow significantly over time. This is also predicted by the derived expressions (15) and (30), which show that the asymptotic $E(\Delta\text{SOC})$ and $\sigma^2(\Delta\text{SOC})$ are independent of time $t$. The reason is that the model is observable [26] and hence the Kalman filter and the least-squares method could stabilize the estimation error and keep it bounded. This is a major benefit of choosing the closed-loop estimation methods over the open-loop coulomb counting. When coulomb counting is used, the SOC estimation error will keep growing over time under the influence of the current sensing bias on top of the initial error. The error could not be corrected until the BMS gets the chance of performing OCV-based SOC resetting after long idling. For the NMC battery under the noise specs considered in this paper, the accumulated SOC estimation error over the cycle will be 5.8%. Given an initial error of 5%, the final error will be 10.8%. According to Fig. 6, the estimation errors of the closed-loop methods are much smaller, with the maximum around 5.1% (instantaneously caused by both sensor noise and model uncertainty) and final values around 1.4%. Since it is possible for the actual EV operation to last for multiple hours before having the chance of SOC resetting, the advantage of the closed-loop methods can be even larger. Nevertheless, for the closed-loop methods, the estimation error depends on the sensor noise level and battery parameters, e.g., OCV slope $\alpha$. If the noise is prominent, or the battery OCV curve is flat, the estimation error could be significantly larger. For example, for the $LiFePO_4$ battery, whose OCV slope is roughly 1/4 of that of the NMC battery, the estimation error can be four times as large.

It is noted that Fig. 6 presents the SOC estimation errors caused by both the (injected) sensor noises and the model uncertainty shown in Fig. 5. It would be interesting to compare the contribution of the two error sources. The comparison is presented in Fig. 7, where the solid line indicates the overall SOC estimation error, the dotted line represents the error caused by sensor noises, and the dashed line denotes the error caused by model uncertainty. When calculating the sensor-noise-induced error, the SOC estimation is performed after the model uncertainty is compensated (subtracted from the voltage measurement). For the computation of the model-uncertainty-induced error, the estimation is conducted using the current and voltage measurement data without the injected sensor noises. It is seen from Fig. 7 that the sensor noises and the model uncertainty have about the same contribution toward the total SOC estimation error under the investigated drive cycle. The average error caused by the sensor noises is 1.5% and the maximum is 2.9%, while those caused by the model uncertainty are 0.9% and 2.9%, respectively. The sensor-noise-induced error is relatively steady, varying mildly over the cycle due to minor change in the OCV slope of the NMC battery. The model-uncertainty-induced error fluctuates more drastically as dictated by the varying magnitude

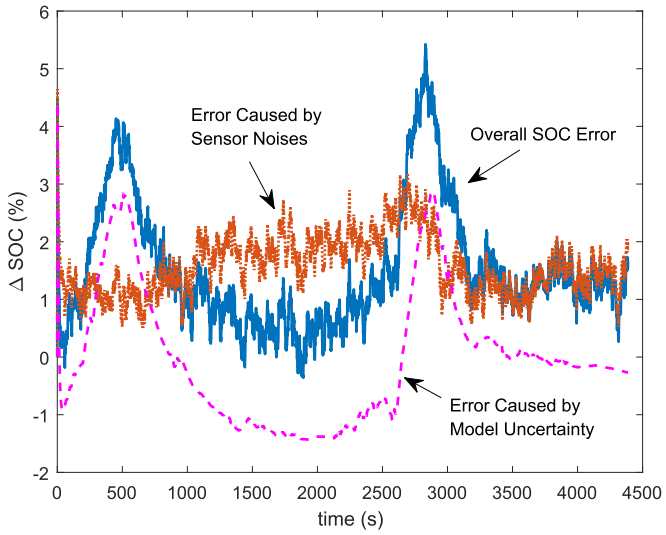


Fig. 7. Comparison of SOC Estimation Error Caused by Sensor Noises and Model Uncertainty.

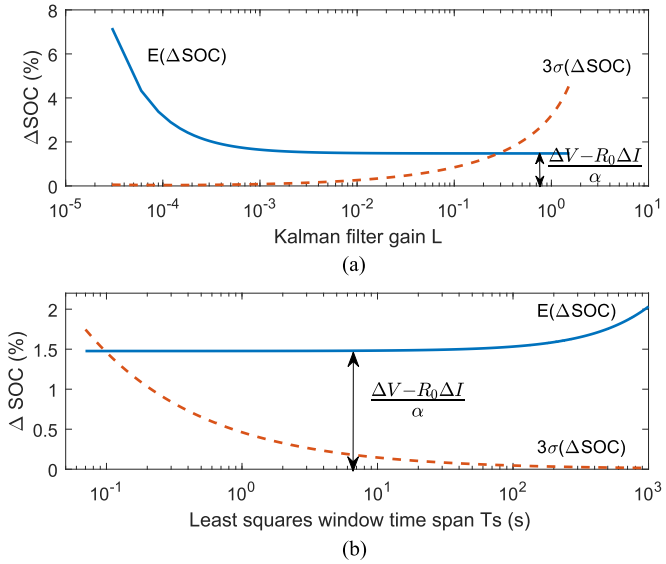


Fig. 8. Asymptotic $E(\Delta\mathrm{SOC})$ and $3\sigma(\Delta\mathrm{SOC})$ of (a) Kalman filter and (b) least-squares under different values of observer tuning parameter.

of the model uncertainty shown in Fig. 5. Both errors are not negligible and need to be cautioned by the battery management system. Under the combined effect of these two error sources, the total SOC estimation error peaks at 5.1% at around 2800 s.

## V. Impact of Observer Parameter Tuning on SOC Estimation Error

In this section, the dependency of the estimation bias $E(\Delta\mathrm{SOC})$ and the variance $\sigma^2(\Delta\mathrm{SOC})$ on observer parameters is investigated.

For the Kalman filter, the magnitude of $E(\Delta\mathrm{SOC})$ and $3\sigma(\Delta\mathrm{SOC})$ under a wide range of gain $L$ is shown in Fig. 8(a). The results are calculated based on the analytic expressions derived in (30). The parameters of the NMC battery are used for calculation, i.e., $R_0 = 2$ mΩ and $C_{\mathrm{bat}} = 5$ Ah. The value of $\alpha$ is set to 0.65 V/100% SOC since for this battery, the OCV slope is close to be constant at this value in the nominal operation range of 10–100% SOC [35]. The gain $L$ varies between $3 \times 10^{-5}$ and 1.54, which corresponds to varying the process variance $Q$ between $10^{-8}$ and $10^{7}$ while fixing the measurement variance $R$ at 10. It is seen from Fig. 8(a) that $E(\Delta\mathrm{SOC})$ and $3\sigma(\Delta\mathrm{SOC})$ exhibit opposite trends as $L$ increases. The bias $E(\Delta\mathrm{SOC})$ decreases as $L$ grows, and reaches a plateau at $\frac{\Delta V - R_0 \Delta I}{\alpha}$ eventually. The plateau represents the fundamental estimation bias that cannot be mitigated by gain tuning. Meanwhile, $3\sigma(\Delta\mathrm{SOC})$ starts to grow significantly after $L$ gets above $10^{-2}$. This tradeoff regarding suppressing the estimation bias and variance agrees with the theoretic discussion in Section III-B. The bias $E(\Delta\mathrm{SOC})$ dominates the estimation error when $L$ is small, while $3\sigma(\Delta\mathrm{SOC})$ becomes dominant under large $L$. The optimal $L$ that balances the estimation bias and variance can be determined based on the accuracy requirement. For the least-squares method, the magnitude of $E(\Delta\mathrm{SOC})$ and $3\sigma(\Delta\mathrm{SOC})$ under a wide range of estimation window span $T_s$ is shown in Fig. 8(b). The value of $T_s$ is related to the number of data points $N$ as $T_s = N\Delta t$. Similar to the Kalman filter, $E(\Delta\mathrm{SOC})$ and $3\sigma(\Delta\mathrm{SOC})$ show opposite dependency on the tuning parameter $T_s$. The bias $E(\Delta\mathrm{SOC})$ increases with $T_s$, and there is a fundamental bias $\frac{\Delta V - R_0 \Delta I}{\alpha}$ that cannot be reduced even if the window is arbitrarily small. At the same time, $3\sigma(\Delta\mathrm{SOC})$ decreases monotonically with $T_s$. This tradeoff is also in accordance with the theoretical discussion in Section III-A. The optimal $T_s$ can be chosen to balance the estimation bias and variance based on requirement.

## VI. Conclusion

This paper establishes the theoretical relationship between the battery SOC estimation error and the voltage and current sensor noises. Important findings have been made for closed-loop observer tuning. For both the Kalman filter and the least-squares method, there exists a tradeoff between suppressing the bias and the variance of SOC estimation. For the Kalman filter, applying large observer gain reduces the estimation bias but at the cost of increasing the variance. The estimation bias dominates the estimation error when the gain is small, while the variance becomes dominant under a large gain. Similarly, for the least-squares method, increasing the number of data points (or the time span) of the estimation window reduces the estimation bias but increases the variance. More interestingly, it is also found that there exists a fundamental estimation bias that could not be mitigated through observer tuning. The magnitude of the fundamental bias is $\frac{\Delta V - \Delta I R_0}{\alpha}$ for both methods. In addition, the estimation variance derived under biased estimation is shown as identical to the Cramer–Rao bound derived previously for unbiased estimation.

The results obtained in this paper could benefit battery SOC estimation in multiple aspects. First, the analytic expressions can be used to evaluate and predict the SOC estimation errors conveniently. Since it is often extremely difficult, if not impossible, to eradicate the estimation errors caused by sensing

noises in practice, the robustness and reliability of SOC estimation become critical concerns. The predicted estimation bias and variance will provide valuable information for reliability evaluation and facilitate robust control and uncertainty management. Second, the identified relationship between the estimation error and the observer tuning parameter could aid the observer design process. Traditionally, the Kalman filter needs to assume a process noise with known covariance to calculate the observer gain. The physical insight of the process noise is often unclear, making it hard to determine the covariance. By using the derived error expressions, a new observer design method might be proposed, to optimize/balance the estimation bias and variance caused by sensor noises. The physical significance of sensor noises is easily understood and the noise characteristics can be practically determined.

## REFERENCES


[1] C.-C. Lin, H. Peng, J. W. Grizzle, and J.-M. Kang, "Power management strategy for a parallel hybrid electric truck," *IEEE Trans. Control Syst. Technol.*, vol. 11, no. 6, pp. 839–849, Nov. 2003.

[2] Y. Gao and M. Ehsani, "Design and control methodology of plug-in hybrid electric vehicles," *IEEE Trans. Ind. Electron.*, vol. 57, no. 2, pp. 633–640, Feb. 2010.

[3] S. N. Motapon, L.-A. Dessaint, and K. Al-Haddad, "A comparative study of energy management schemes for a fuel-cell hybrid emergency power system of more-electric aircraft," *IEEE Trans. Ind. Electron.*, vol. 61, no. 3, pp. 1320–1334, Mar. 2014.

[4] H. Perez, X. Hu, S. Dey, and S. Moura, "Optimal charging of li-ion batteries with coupled electro-thermal-aging dynamics," *IEEE Trans. Veh. Technol.*, vol. 66, no. 9, pp. 7761–7770, Sep. 2017.

[5] M. Vasiladiotis and A. Rufer, "A modular multiport power electronic transformer with integrated split battery energy storage for versatile ultrafast EV charging stations," *IEEE Trans. Ind. Electron.*, vol. 62, no. 5, pp. 3213–3222, May 2015.

[6] H. Wang, S. Dusmez, and A. Khaligh, "Maximum efficiency point tracking technique for $llc$-based PEV chargers through variable DC link control," *IEEE Trans. Ind. Electron.*, vol. 61, no. 11, pp. 6041–6049, Nov. 2014.

[7] C. Speltino, A. Stefanopoulou, and G. Fiengo, "Cell equalization in battery stacks through state of charge estimation polling," in *Proc. IEEE Am. Control Conf.*, 2010, pp. 5050–5055.

[8] S. J. Moura, J. C. Forman, S. Bashash, J. L. Stein, and H. K. Fathy, "Optimal control of film growth in lithium-ion battery packs via relay switches," *IEEE Trans. Ind. Electron.*, vol. 58, no. 8, pp. 3555–3566, Aug. 2011.

[9] K. Kutluay, Y. Cadirci, Y. S. Ozkazanc, and I. Cadirci, "A new online state-of-charge estimation and monitoring system for sealed lead-acid batteries in telecommunication power supplies," *IEEE Trans. Ind. Electron.*, vol. 52, no. 5, pp. 1315–1327, Oct. 2005.

[10] K. Ng, C. Moo, Y. Chen, and Y. Hsieh, "Enhanced coulomb counting method for estimating state-of-charge and state-of-health of lithium-ion batteries," *Appl. Energy*, vol. 86, no. 9, pp. 1506–1511, 2004.

[11] G. L. Plett, "Extended kalman filtering for battery management systems of LIPB-based HEV battery packs part 3. State and parameter estimation," *J. Power Sources*, vol. 134, pp. 277–292, 2004.

[12] A. M. Bizeray, S. Zhao, S. R. Duncan, and D. A. Howey, "Lithium-ion battery thermal-electrochemical model-based state estimation using orthogonal collocation and a modified extended kalman filter," *J. Power Sources*, vol. 296, pp. 400–412, 2015.

[13] D. D. Domenico, A. Stefanopoulou, and G. Fiengo, "Lithium-ion battery state of charge and critical surface charge estimation using an electrochemical model-based extended kalman filter," *J. Dyn. Syst., Meas., Control*, vol. 132, pp. 061302–061313, 2010.

[14] M. Charkhgard and M. Farrokhi, "State-of-charge estimation for lithium-ion batteries using neural networks and EKF," *IEEE Trans. Ind. Electron.*, vol. 57, no. 12, pp. 4178–4187, Dec. 2010.

[15] R. Xiong, F. Sun, Z. Chen, and H. He, "A data-driven multi-scale extended kalman filtering based parameter and state estimation approach of lithium-ion polymer battery in electric vehicles," *Appl. Energy*, vol. 113, pp. 463–476, 2014.

[16] H. Fang *et al.*, "Improved adaptive state-of-charge estimation for batteries using a multi-model approach," *J. Power Sources*, vol. 254, pp. 258–267, 2014.

[17] H. Rahimi-Eichi, F. Baronti, and M.-Y. Chow, "Online adaptive parameter identification and state-of-charge coestimation for lithium-polymer battery cells," *IEEE Trans. Ind. Electron.*, vol. 61, no. 4, pp. 2053–2061, Apr. 2014.

[18] M. Coleman, C. K. Lee, C. Zhu, and W. G. Hurley, "State-of-charge determination from EMF voltage estimation: Using impedance, terminal voltage, and current for lead-acid and lithium-ion batteries," *IEEE Trans. Ind. Electron.*, vol. 54, no. 5, pp. 2550–2557, Oct. 2007.

[19] X. Lin, A. G. Stefanopoulou, Y. Li, and R. D. Anderson, "State of charge estimation of cells in series connection by using only the total voltage measurement," in *Proc. Am. Control Conf.*, 2013, pp. 704–709.

[20] X. Lin, A. G. Stefanopoulou, Y. Li, and R. D. Anderson, "State of charge imbalance estimation for battery strings under reduced voltage sensing," *IEEE Trans. Control Syst. Technol.*, vol. 23, no. 3, pp. 1052–1062, May 2015.

[21] F. Zhang, G. Liu, L. Fang, and H. Wang, "Estimation of battery state of charge with $H\infty$ observer: Applied to a robot for inspecting power transmission lines," *IEEE Trans. Ind. Electron.*, vol. 59, no. 2, pp. 1086–1095, Feb. 2012.

[22] Y.-S. Lee, W.-Y. Wang, and T.-Y. Kuo, "Soft computing for battery state-of-charge (BSOC) estimation in battery string systems," *IEEE Trans. Ind. Electron.*, vol. 55, no. 1, pp. 229–239, Jan. 2008.

[23] S. J. Moura, N. A. Chaturvedi, and M. Krstic, "Adaptive partial differential equation observer for battery state-of-charge/state-of-health estimation via an electrochemical model," *J. Dyn. Syst., Meas., Control*, vol. 136, no. 1, pp. 011015-1–011015-8, 2014.

[24] S. Dey, B. Ayalew, and P. Pisu, "Nonlinear robust observers for state-of-charge estimation of lithium-ion cells based on a reduced electrochemical model," *IEEE Trans. Control Syst. Technol.*, vol. 23, no. 5, pp. 1935–1942, Sep. 2015.

[25] M. Gholizadeh and F. R. Salmasi, "Estimation of state of charge, unknown nonlinearities, and state of health of a lithium-ion battery based on a comprehensive unobservable model," *IEEE Trans. Ind. Electron.*, vol. 61, no. 3, pp. 1335–1344, Mar. 2014.

[26] S. Zhao, S. R. Duncan, and D. A. Howey, "Observability analysis and state estimation of lithium-ion batteries in the presence of sensor biases," *IEEE Trans. Control Syst. Technol.*, vol. 25, no. 1, pp. 326–333, Jan. 2017.

[27] Z. Liu, Q. Ahmed, J. Zhang, G. Rizzoni, and H. He, "Structural analysis based sensors fault detection and isolation of cylindrical lithium-ion batteries in automotive applications," *Control Eng. Practice*, vol. 52, pp. 46–58, 2016.

[28] S. Mendoza, J. Liu, P. Mishra, and H. Fathy, "On the relative contributions of bias and noise to lithium-ion battery state of charge estimation errors," *J. Energy Storage*, vol. 11, pp. 86–92, 2017.

[29] X. Lin, A. Stefanopoulou, P. Laskowsky, J. Freudenberg, Y. Li, and R. D. Anderson, "State of charge estimation error due to parameter mismatch in a generalized explicit lithium ion battery model," in *Proc. ASME Dyn. Syst. Control Conf. Bath/ASME Symp. Fluid Power Motion Control*, 2011, pp. 393–400.

[30] P. P. Mishra, M. Garg, S. Mendoza, J. Liu, C. D. Rahn, and H. K. Fathy, "How does model reduction affect lithium-ion battery state of charge estimation errors? Theory and experiments," *J. Electrochem. Soc.*, vol. 164, no. 2, pp. A237–A251, 2017.

[31] V. Ramadesigan, K. Chen, N. A. Burns, V. Boovaragavan, R. D. Braatz, and V. R. Subramanian, "Parameter estimation and capacity fade analysis of lithium-ion batteries using reformulated models," *J. Electrochem. Soc.*, vol. 158, no. 9, pp. A1048–A1054, 2011.

[32] J. Vazquez-Arenas, L. E. Gimenez, M. Fowler, T. Han, and S.-K. Chen, "A rapid estimation and sensitivity analysis of parameters describing the behavior of commercial li-ion batteries including thermal analysis," *Energy Convers. Manage.*, vol. 87, pp. 472–482, 2014.

[33] J. C. Forman, S. J. Moura, J. L. Stein, and H. K. Fathy, "Genetic identification and Fisher identifiability analysis of the Doyle–Fuller–Newman model from experimental cycling of a LIFEPO 4 cell," *J. Power Sources*, vol. 210, pp. 263–275, 2012.

[34] A. Sharma and H. K. Fathy, "Fisher identifiability analysis for a periodically-excited equivalent-circuit lithium-ion battery model," in *Proc. IEEE Am. Control Conf.*, 2014, pp. 274–280.

[35] X. Lin and A. G. Stefanopoulou, "Analytic bound on accuracy of battery state and parameter estimation," *J. Electrochem. Soc.*, vol. 162, no. 9, pp. A1879–A1891, 2015.

[36] X. Lin, "Analytic analysis of the data-dependent estimation accuracy of battery equivalent circuit dynamics," *IEEE Control Syst. Lett.*, vol. 1, no. 2, pp. 304–309, 2017.
[37] X. Lin, "On the analytic accuracy of battery SoC, capacity and resistance estimation," in *Proc. Am. Control Conf.*, 2016, pp. 4006–4011.
[38] F. Auger, M. Hilairet, J. M. Guerrero, E. Monmasson, T. Orlowska-Kowalska, and S. Katsura, "Industrial applications of the Kalman filter: A review," *IEEE Trans. Ind. Electron.*, vol. 60, no. 12, pp. 5458–5471, Dec. 2013.
[39] X. Lin, "Analytic analysis of battery SoC estimation error under sensor noises," in *Proc. IFAC 2017 World Congr.*, 2017, pp. 2175–2180.
[40] X. Hu, F. Sun, and Y. Zou, "Estimation of state of charge of a lithium-ion battery pack for electric vehicles using an adaptive Luenberger observer," *Energies*, vol. 3, no. 9, pp. 1586–1603, 2010.
[41] X. Hu, S. Li, and H. Peng, "A comparative study of equivalent circuit models for li-ion batteries," *J. Power Sources*, vol. 175, pp. 359–367, 2012.
[42] L.-R. Chen, S.-L. Wu, D.-T. Shieh, and T.-R. Chen, "Sinusoidal-ripple-current charging strategy and optimal charging frequency study for li-ion batteries," *IEEE Trans. Ind. Electron.*, vol. 60, no. 1, pp. 88–97, Jan. 2013.
[43] X. Lin *et al.*, "A lumped-parameter electro-thermal model for cylindrical batteries," *J. Power Sources*, vol. 257, pp. 1–11, 2014.
[44] L. Lu, X. Han, J. Li, J. Hua, and M. Ouyang, "A review on the key issues for lithium-ion battery management in electric vehicles," *J. Power Sources*, vol. 226, pp. 272–288, 2013.
[45] M. Klein, S. Tong, and J. Park, "In-plane nonuniform temperature effects on the performance of a large-format lithium-ion pouch cell," *Appl. Energy*, vol. 165, pp. 639–647, 2016.
[46] N. A. Samad, J. B. Siegel, and A. G. Stefanopoulou, "Parameterization and validation of a distributed coupled electro-thermal model for prismatic cells," in *Proc. ASME Dyn. Syst. Control Conf.*, 2014, pp. V002T23A006–V002T23A014.
[47] S. M. M. Alavi, A. Mahdi, S. J. Payne, and D. A. Howey, "Identifiability of generalized randles circuit models," *IEEE Trans. Control Syst. Technol.*, vol. 25, no. 6, pp. 2112–2120, Nov. 2017.
[48] O. Abdel-baqi, A. Nasiri, and P. Miller, "Dynamic performance improvement and peak power limiting using ultracapacitor storage system for hydraulic mining shovels," *IEEE Trans. Ind. Electron.*, vol. 62, no. 5, pp. 3173–3181, May 2015.
[49] Y. Parvini, J. B. Siegel, A. G. Stefanopoulou, and A. Vahidi, "Supercapacitor electrical and thermal modeling, identification, and validation for a wide range of temperature and power applications," *IEEE Trans. Ind. Electron.*, vol. 63, no. 3, pp. 1574–1585, Mar. 2016.
[50] J. Marcicki, M. Canova, A. T. Conlisk, and G. Rizzoni, "Design and parametrization analysis of a reduced-order electrochemical model of graphite/lifepo 4 cells for SOC/SOH estimation," *J. Power Sources*, vol. 237, pp. 310–324, 2013.
[51] T. K. Dong, A. Kirchev, F. Mattera, and Y. Bultel, "Modeling of lithium iron phosphate batteries by an equivalent electrical circuit: Method of model parameterization and simulation," *ECS Trans.*, vol. 25, no. 35, pp. 131–138, 2010.
[52] G. K. Prasad and C. D. Rahn, "Reduced order impedance models of lithium ion batteries," *J. Dyn. Syst., Meas., Control*, vol. 136, no. 4, 2014, Art. no. 041012.
[53] P. E. Jacob, S. M. M. Alavi, A. Mahdi, S. J. Payne, and D. A. Howey, "Bayesian inference in non-Markovian state-space models with applications to battery fractional-order systems," *IEEE Trans. Control Syst. Technol.*, 2017, doi: 10.1109/TCST.2017.2672402.
[54] T. F. Fuller, M. Doyle, and J. Newman, "Simulation and optimization of the dual lithium ion insertion cell," *J. Electrochem. Soc.*, vol. 141, no. 1, pp. 1–10, Jan. 1994.

**Xinfan Lin** (M'17) received the B.S. and M.S. degrees in automotive engineering from Tsinghua University, Beijing, China, in 2007 and 2009, respectively, and the Ph.D. degree in mechanical engineering from the University of Michigan, Ann Arbor, MI, USA, in 2014.

He is currently an Assistant Professor with the Department of Mechanical and Aerospace Engineering, University of California, Davis, CA, USA. From 2014–2016, he was a Research Engineer at Ford Motor Company, responsible for the development of the battery management system and other EV components and systems. He has published more than 20 peer-reviewed papers and received two patents. His research interests include modeling, estimation and control with applications in energy and automotive systems.